

©Copyright 2015

Jungsoo Park

Development and Investigation of a Dihydroartemisinin-Resistant Human  
Leukemia Cell Line

Jungsoo Park

A thesis submitted in partial fulfillment of the requirements for the degree of

Master of Science in Bioengineering

University of Washington

2015

Supervisory Committee:

Narendra Pal Singh

Henry Lai

Program authorized to Offer Degree:

Department of Bioengineering

University of Washington

## Abstract

Development and Investigation of a Dihydroartemisinin-Resistant Human Leukemia Cell Line

Jungsoo Park

Chair of the Supervisory Committee:

Narendra Pal Singh, MBBS, MS

Artemisinin generates cytotoxic free radicals when it reacts with ferrous iron, and induces molecular damages and apoptosis in cells. Its toxicity is more selective toward cancer cells because cancer cells contain a higher level of intracellular free iron. Dihydroartemisinin (DHA), an active metabolite of artemisinin, has selective cytotoxicity toward Molt-4 human lymphoblastoid cells and could be a potent cancer chemotherapeutic compound. A major concern is whether cancer cells could develop resistance to DHA after repeated administrations, thus limiting its therapeutic efficacy. In the present study, a DHA-resistant Molt-4 cell line (RTN) was developed by exposing Molt-4 cells to gradually increasing concentrations of DHA *in vitro*. The half maximal inhibitory concentration (IC<sub>50</sub>) of DHA for RTN cells was significantly higher than that of Molt-4 cells. However, RTN cells did not exhibit any significant cross resistance to artemisinin-tagged holotransferrin (ART-TF), a synthetic artemisinin compound. In addition, DNA damage induced by DHA and ART-TF in both Molt-4 and RTN cells was investigated using the Comet assay. RTN cells exhibited a significantly lower level of basal and X-ray induced DNA damage compared to Molt-4 cells. Both DHA and ART-TF induced DNA damage

in normal Molt-4 cells, whereas DNA damage was induced in RTN cells by ART-TF, and not DHA. This research shows that ART-TF is a potent anticancer agent against DHA- resistant RTN cells and could be used as a replacement when resistance to DHA is developed.

## Contents

List of Figures .....	i
Introduction.....	1
Materials and Methods.....	4
Development of a DHA-resistant RTN cell line.....	4
Synthesis of Artemisinin-tagged holotransferrin (ART-TF) .....	4
The Comet Assay.....	9
Results.....	13
Time-response plots of different concentrations of DHA.....	13
Dose-responses to DHA of Molt-4 and RTN cells .....	13
Dose responses to ART-TF of Molt-4 and RTN cells .....	14
Basal and X-ray-induced DNA damage in Molt-4 and RTN cells .....	15
DNA damaging effect of DHA and ART-TF on Molt-4 cells.....	19
DNA damaging effect of DHA and ART-TF on RTN cells.....	19
Discussion.....	21
Conclusion .....	25
Acknowledgment .....	26
Copyright Note.....	26
References.....	27

## List of Figures

**Figure 1:** Synthesis of artelinic acid hydrazide. **Page 6**

**Figure 2:** Synthesis of artelinate-tagged transferrin. **Page 7**

**Figure 3:** Time-response plots for different concentrations of Molt-4 and RTN cells. **Page 14**

**Figure 4:** Log dose–response plots for Molt-4 cells and RTN cells to dihydroartemisinin (DHA) at the 24-h and 48-h time point. **Page 15**

**Figure 5:** Log dose–response plots for Molt-4 cells and RTN cells to artemisinin-tagged holotransferrin (ART-TF) at the 24-h and 48-h time point. **Page 16**

**Figure 6:** Mean ‘tail moment’ and mean ‘tail integrated intensity’ of the four treatment groups: Molt-4 control, X-ray-treated Molt-4, RTN control, and X-ray-treated RTN. **Page 17**

**Figure 7:** Comet images of Molt-4 Control, RTN Control, Molt-4 X-Ray and RTN X-Ray that closely match each treatment’s mean ‘tail moment’ and mean ‘tail integrated intensity’. **Page 18**

**Figure 8:** Mean ‘tail moment’ and mean ‘tail integrated intensity’ of control Molt-4 cells and those treated with dihydroartemisinin (DHA) and artemisinin-tagged holotransferrin (ART-TF) for 24 h. **Page 20**

**Figure 9:** Comet images of Molt-4 Control, Molt-4 DHA, and Molt-4 ART-TF that closely match each treatment’s mean ‘tail moment’ and mean ‘tail integrated intensity’. **Page 21**

**Figure 10:** Mean ‘tail moment’ and mean ‘tail integrated intensity’ of control RTN cells and those treated with dihydroartemisinin (DHA) and artemisinin-tagged holotransferrin (ART-TF) for 24 h. **Page 22**

**Figure 11:** Comet images of RTN Control, RTN DHA and RTN ART-TF that closely match each treatment’s mean ‘tail moment’ and mean ‘tail integrated intensity’. **Page 23**

## Introduction

Artemisinin, a renowned anti-malarial compound extracted from the plant *Artemisia annua L* (sweet wormwood)(1). Interestingly, in addition to the anti-malarial property, artemisinin and its derivatives also have been reported to exhibit anticancer properties *in vitro* (2-4), *in vivo* (5,6) and in cancer patients (7,8). Further research has shown that dihydroartemisinin (DHA), a major active metabolite form of artemisinin, has selective anticancer activity against Molt-4 human lymphoblastic leukemia cells by inducing apoptosis (9).

Artemisinin contains an endoperoxide moiety which reacts with intracellular free ferrous irons to generate carbon-based free radicals. When these carbon-based radicals are formed in an intracellular environment, they can induce macromolecular damages, including DNA damage, which eventually account for artemisinin and its derivatives' cytotoxicity (10). In mammalian cells, iron is transported to the cell *via* receptor-mediated endocytosis of the iron-carrying plasma protein holotransferrin (iron-loaded transferrin) (11). When the pH level decreases in an endosome, iron is released from holotransferrin and then pumped out into the cell's cytoplasm. Afterwards, transferrin and transferrin receptors are recycled back to the cell surface. Since cancer cells require larger amount of iron for rapid cell division and proliferation (12, 13), they express higher level of transferrin receptors on their cell surface and uptake a higher amount of iron. Therefore, higher intracellular iron level of cancer cells would make them more vulnerable to artemisinin cytotoxicity compared to normal cells. Because of its high specific cytotoxic effect against cancer cells, artemisinin and its derivatives, including DHA, are potential effective cancer chemotherapeutic drugs.

However, a major issue with chemotherapy is that cancer cells could potentially develop drug resistance. Drug resistance is a problem to a majority of the anticancer agents; therefore, it is highly plausible that cancer cells could also develop resistance to DHA and other artemisinin derivative compounds after repeated administrations. Increased drug efflux, enhanced drug inactivation, apoptosis defects, insufficient drug delivery, target-receptor modification, increased tolerance to DNA damage, or increased DNA damage repair might contribute to the biological mechanisms of drug resistance of cancer cells to anti-cancer agents (14-19).

In an effort to overcome resistance to DHA, experimental studies using *in vitro* models of DHA-resistant cancer cell lines and investigating cell viability and DNA damage in human cancer cell lines in response to artemisinin-like compounds might provide insight into the effective usage of artemisinin and its derivatives (20). Also, synthetic artemisinin derivatives which have been reported to exhibit enhanced anticancer properties compared to DHA (21) can be potential candidates to kill DHA-resistant cancer cells and replacements once resistance has developed.

One of the most potent synthetic artemisinin derivatives known is artemisinin-tagged holotransferrin (ART-TF) developed by Lai *et al.* (22). Lai *et al.* reported that ART-TF, when compared to DHA, was more potent in killing Molt-4 cells. In ART-TF, artemisinin is covalently attached to holotransferrin, where artemisinin can be co-transported into the cells via receptor mediated endocytosis whereas DHA enters the cell by diffusion across the cell membrane. Because ART-TF is delivered through the cells by different mechanism of action, ART-TF might be utilized as a potential anticancer agent to overcome the DHA-resistance in cancer cells.



The most renowned method for assessing DNA damage is the Comet assay (microgel electrophoresis) (23). The major advantage of the Comet assay over other DNA-damage measurement methods is that it has the capability to assess DNA damage at single-cell level. Another feature of the Comet assay is that it has the sensitivity for detecting low levels of DNA damage (24, 25). In addition, only a small number of cells are necessary for the assay allowing analysis of DNA damage of various experimental conditions within a short period of time.

Hence in the present thesis, DHA-resistant Molt-4 cell line (RTN) was established by continuously exposing Molt-4 human lymphoblastic leukemia cells to gradually increasing concentrations of DHA *in vitro*. Characteristics of the Molt-4 and RTN cells were examined and their responses to DHA were compared. Then, Molt-4 and RTN cells were tested with ART-TF to compare its potency with DHA. In addition, to investigate the levels of DNA damage induced by DHA and ART-TF in both Molt-4 and RTN cells, the alkaline Comet assay, which quantifies DNA single-strand breaks in cells, was performed. In the Comet assay, single cells with significant levels of DNA damage display an increased migration of DNA from the nucleus under electrophoresis (26). Analysis of single cells based on size and the intensity of the comet tail provides a comparative index of DNA damage induced by DHA and ART-TF on Molt-4 and RTN cells.

## Materials and Methods

**Chemicals.** All chemicals were purchased from Sigma Aldrich (St Louis, MO, USA) unless stated otherwise.

**Molt-4 cell culture.** Molt-4 cells were purchased from the American Type Culture Collection (ATCC, Manassas, VA, USA). They were cultured in RPMI-1640 (Life Technologies, Grand Island, NY, USA) with 10% fetal bovine serum (ATCC) at 37°C with 5% CO<sub>2</sub> in air and 100% humidity. At a cell density of 6×10<sup>5</sup> cells/ml, Molt-4 cells were diluted to a density of approximately 6×10<sup>4</sup> cells/ml at 24 h prior to experiments.

**Development of a DHA-resistant RTN cell line.** Molt-4 cells were first exposed to 25 μM of DHA (Holley Pharmaceuticals, Chongqing, China) in RPMI-1640 medium for 24 h. Cells then were washed by centrifugation at 870 x g for 5 min in a microfuge (Sorvall Microspin, model 245) to obtain cell pellets. Pellets were re-suspended in fresh RPMI-1640 medium. Until the surviving cells completely recovered to a cell density of 6×10<sup>5</sup> cells/ml and exhibited a normal exponential growth, cells were then treated again with 25 μM of DHA for 24 h. This step was repeated two times more. The cells were then exposed to increase concentrations of DHA: three times each (3 × 24 h) at 50 μM, 75 μM, and 100 μM. After all the steps, the surviving cells were washed and cultured in DHA-free RPMI 1640 medium. The resulting cell line was termed the RTN cell line.

**Synthesis of Artemisinin-tagged holotransferrin (ART-TF)** Artemisinin-tagged holotransferrin (ART-TF) was synthesized as previously described by Lai *et al* (22). The synthesis of ART-TF was divided into three steps.

*Synthesis of methyl 4-[(10-dihydroartemisininoxy) methyl] benzoate of artemisinin.*

Dihydroartemisinin (DHA) was acetylated first with acetic anhydride in pyridine in the presence of 4- (dimethylamino)pyridine as previously described by Kim and Sasaki (27).

In acetylated artemisinin (0.100 gm, 0.306 mmol) (compound 1 in Figure 1) and methyl p-hydroxymethylbenzoate (0.0056 gm, 0.336 mmol) in anhydrous  $\text{CHCl}_3$  (1 ml), Trimethylsilyl-trifluoromethanesulfonate (TMSOT, 0.013 ml, 0.06 mmol) was added and the reaction solution was stirred for 40 min at room temperature. Then, the mixture was quenched with saturated  $\text{NaHCO}_3$  solution (0.5 ml) and was extracted with  $\text{CHCl}_3$ . The organic layer was then washed with water and brine, dried over  $\text{Na}_2\text{SO}_4$  and concentrated under vacuum. The residue obtained was purified by flash chromatography using 20% ethyl acetate/ hexane to produce artelinic acid methyl ester (0.105g, 80%).

*Synthesis of 4-[(10-dihydroartemisininoxy) methyl] benzoic acid hydrazide*

In the artelinic acid methyl ester contained in ethanol solution (0.2 ml) (compound 2 in Figure 1), hydrazine hydrate (0.046 ml) was added and the mixture was heated for 50 °C, for 48 h. The mixture was then concentrated under vacuum and water (2 ml) was added, and then extracted with  $\text{CHCl}_3$ . The organic extracts were then dried over  $\text{Na}_2\text{SO}_4$ , concentrated under vacuum and the crude product acquired was purified by flash column chromatography using 4% methanol/ $\text{CHCl}_3$  to eventually obtain artelinic acid hydrazide.

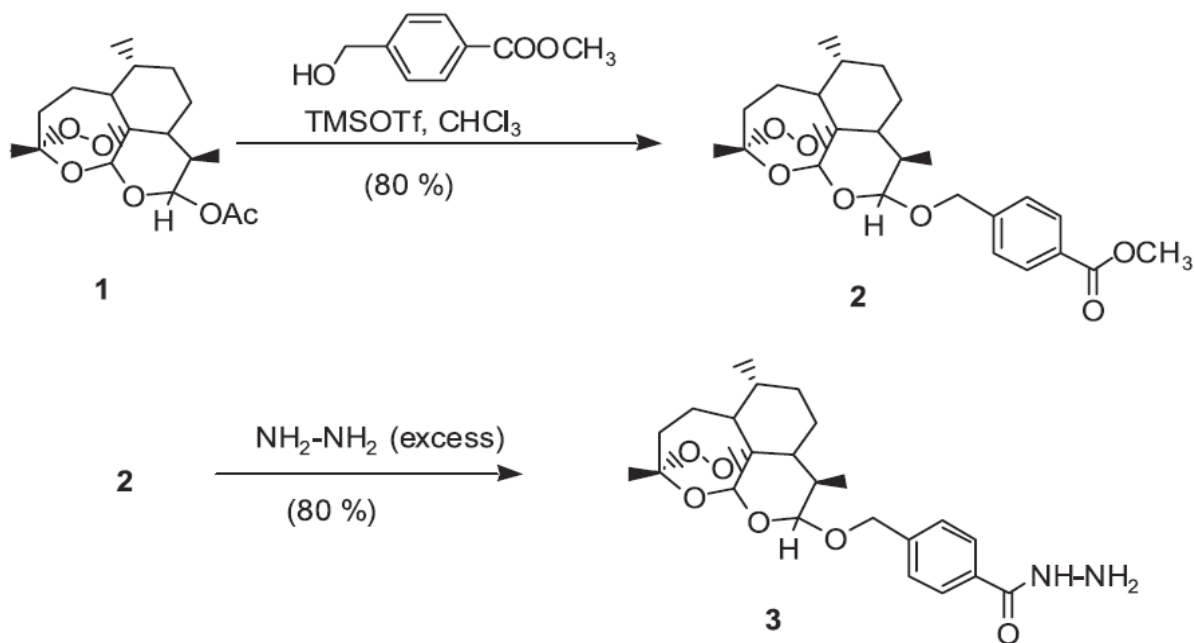


**Figure 1. Synthesis of artelinic acid hydrazide (3) from dihydroartemisinin (1). Artelinic acid ester (2) is the intermediate compound (22).**

### *Oxidation of transferrin*

Human holotransferrin (1g) was dissolved in 50 ml, 0.1 M sodium acetate (pH 5.5) and then it was incubated at room temperature with 15 ml, 50 mM sodium periodate (NaIO<sub>4</sub>) for 30 min. Afterwards, using the Sephadex G-25 column equipped with a UV detector, the holotransferrin mixture was eluted with 0.1 M sodium acetate pH 5.5 in a cold room. Holotransferrin was then oxidized with 50 mM NaIO<sub>4</sub> before tagging with artelinic acid hydrazine to give the final product artemisinin-tagged holotransferrin. DPBS saline buffer was used as an eluent. Protein containing fractions were gathered to give the final product artelinic tagged-transferrin (artemisinin tagged holotransferrin, ART-TF).

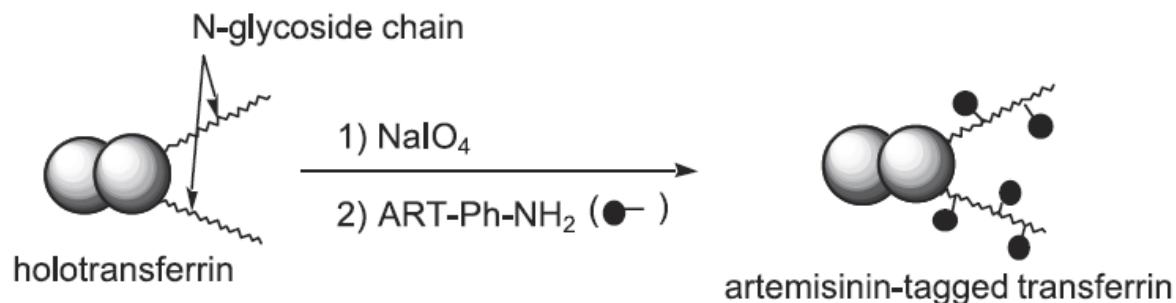


**Figure 2.** Synthesis of artemisinin-tagged transferrin. The two black circles represent the N- and the C- terminal domains of transferrin. These two domains were oxidized with  $\text{NaIO}_4$  and then conjugated with artemisinin acid hydrazide (22).

*Conjugation of oxidized transferrin with artemisinin hydrazide (Figure 2)*

Artemisinin hydrazide (0.120 gm) dissolved in DMSO (7.8 ml) solution (compound 3 in Figure 1) was added to the oxidized transferrin (60 ml) and the reaction mixture was incubated at room temperature for 2 h. In a cold room, Sephadex G-25 column equipped with a UV monitor was used to remove low molecular weight reagents and byproducts from the reaction by gel filtration.

**Drug testing on Molt-4 and RTN cells.** Molt-4 and RTN cells were pre-cultured for 24 h to allow the cells and the RPMI-1640 media to be conditioned before drug treatment at a density ranging from  $1 \times 10^5 \sim 1.5 \times 10^5$  cells/ml. Cells were placed (1 ml each) into microfuge tubes prior to drug treatment. At this time, cells were in the log phase of growth. Molt-4 and RTN cells were treated with DHA and ART-TF.

To compare the cytotoxicity of DHA and ART-TF on Molt-4 and RTN cells, cells were incubated with different concentrations of: DHA (12.5, 25, 50, 75, and 100  $\mu$ M) or ART-TF (1, 2, and 4  $\mu$ M). Control samples had no drug treatment. Dihydroartemisinin was dissolved in dimethyl sulfoxide (DMSO) and ART-TF in phosphate-buffered saline (PBS) before adding to cell samples. The final concentration of DMSO and PBS in samples was 1% and 10%, respectively. Similar amounts of the solvents were added to the control samples. Molt-4 and RTN cell numbers were counted using a hemocytometer immediately prior to drug treatment (0 h) and at 24 and 48 h of drug treatment. To assess cell viability, we used trypan blue exclusion. Only viable cells were counted.

**Data analysis of drug testing on Molt-4 and RTN cells.** All experiments were performed three times. The mean and standard deviation were calculated. Responses were calculated as the ratio of viable cell counts at 24 and 48 h time points relative to the viable cell count at 0 h. Log dose–response and time–response curves were plotted using the cell count ratios. The GraphPad Prism 6.03 software (La Jolla, CA, USA) was used for statistical analysis. Time response curves were compared by the method of Krauth (28). The  $a_0$  of the orthogonal polynomial coefficient of the curves, were compared using the Mann–Whitney U-test. Log dose–response curves of drug treatment were plotted. Half maximal inhibitory concentrations ( $IC_{50}$ s) were determined and compared using the two-tailed Student’s *t*-test. A difference at  $p < 0.05$  was considered statistically significant.

**Treatment of Molt-4 and RTN cells to assess DNA damage.** Pre-incubated (for 24 h) Molt-4 and RTN cells at a density of  $1 \sim 1.5 \times 10^5$  cells/ml were allocated (1 ml each) into microfuge tubes prior to drug treatment. At this time, cells were in the log phase of growth. Molt-4 and RTN cells

were treated with DHA (dissolved in DMSO) and ART-TF (dissolved in PBS). Both Molt-4 and RTN cells had three treatment conditions: control, 6.2  $\mu$ M DHA, and 6.2  $\mu$ M ART-TF. Control samples had no drug treatment. The final concentration of DMSO and PBS in all samples was 1% and 10%, respectively. The cells were incubated with the drugs for 24 h and DNA damage was immediately assayed using the Comet assay.

***The Comet Assay.*** The Comet assay was conducted as previously described (25, 29, 30).

#### *Agarose Preparation*

##### 0.5% agarose

Fifty milligrams of high resolution agarose 3:1 (AMRESCO Inc., Solon, OH, USA) were boiled in 10 ml of distilled water in a microwave oven and 100  $\mu$ l of 2 M Tris-HCl (pH 7.4) were added. Volume was set to 10 ml by adding distilled water, and the solution was mixed to provide a concentration of 0.5% 3:1 agarose. The agarose was aliquoted in 1.5 ml microfuge tubes and maintained at 55 °C for use.

##### 0.7% agarose

70 mg of high resolution agarose 3:1 (AMRESCO Inc., Solon, OH, USA) was boiled in 9 ml of distilled water in a microwave oven. 1 ml of 10X PBS (containing in 1 litre: 80 g NaCl, 2 g KCl, 2 g  $\text{KH}_2\text{PO}_4$ , 11.5 g anhydrous  $\text{Na}_2\text{HPO}_4$ , 32 g Tris HCl, at pH 7.4) was added and boiled again. Volume was set to 10 ml by adding distilled water, and the solution was mixed to provide a concentration of 0.7% 3:1 agarose. The agarose was aliquoted in 1.5 ml microfuge tubes and maintained at 42 °C for 24 hrs before use.

### *Slide Preparation*

Clear window frosted MGE slides (Mac & Sons Specialty Glass, Mims, FL, USA) were first pre-coated with 100 µl of 0.5% agarose. Two hundred fifty microliters of 0.7% 3:1 agarose were first layered onto the pre-coated slides and covered with a cover glass (24×50 mm<sup>2</sup>, Corning Glass Works, Corning, NY, USA). For the second layer of the microgel, cells from 1 ml of a sample were centrifuged at 870×g for 5 min and the pellet was suspended in 10 µl of fresh RPMI-1640 media and mixed well with 250 µl of 0.7% 3:1 agarose, and 100 µl of this cell agarose mixture were layered on the MGE slide after removing the cover glass. The cover glass was placed over once again after layering. The slides were placed on a cold steel tray on ice for 1 min. The cover glass was then removed once again and a third layer of microgel was made using 250 µl of 0.7% 3:1 agarose.

### *X-ray irradiation of Molt-4 and RTN cells*

After preparation, the slides were kept on ice. One Molt-4 and one RTN cell slide without any drug treatment were immediately irradiated with 200 rad of X-ray using a Kelley-Koett device (Covington, CT, USA) at a rate of 100 rad/min for 2 min. X-ray irradiation was performed to serve as a positive control.

### *Lysis of cells and Electrophoresis*

After taking the cover glasses off, slides were immersed in a pre-warmed lysing solution (1.25M NaCl, 50 mM tetra sodium salt of ethylenediaminetetraacetic acid (EDTA), 10 mM Tris , pH 10 ) in which 0.5 mg/ml of proteinase K (AMRESCO Inc., Solon, OH, USA) and 1 mg/ml of reduced glutathione had been added just before its use. The lysing solution enables removal of most of the proteins, lipids and other cellular macromolecules in the cells on the slides. The cells were



then lysed at 37°C for 1 h. Slides were then placed in an electrophoretic unit (MGE 2222, Ellard Instrumentation, Monroe, WA, USA) with 1L of an electrophoresis buffer ( 300 mM NaOH, 1 mM EDTA, and 0.2% DMSO, pH 13.5 ). The slides were equilibrated for 20 min in this highly alkaline buffer to unwind DNA and to reveal DNA single strand breaks and alkali labile sites. Slides were then electrophoresed at 18V (0.6 V/cm) (480 mA) for 20 min at room temperature. During electrophoresis, the buffer was circulated at a rate of 100 ml/min using a variable-speed peristaltic pump (Control Company, Friendswood, TX, USA).

To prevent additional DNA damage, all Comet assay steps described above were conducted in minimum light.

#### *DNA Precipitation, staining and image analysis*

Slides were immersed in a solution of 2 mg/ml cetyltrimethylammoniumbromide (CTAB) in 40 mM Tris (pH 7.4) for 10 min to neutralize and precipitate small quantities of DNA. This step was repeated once more. Consequently, the slides were immersed in 20 mM Tris (pH 7.4) in 75% ethanol for 10 min to wash off CTAB while maintaining the DNA in a precipitated state. This step was repeated twice more. The slides were then air dried overnight. The slides were stained one at a time with 100 µl of staining solution (composed of 0.25 µM YOYO-1, 0.25 M NaCl and 0.1 M KCl in 2.5% DMSO and 0.5% Sucrose). Images of the comets were captured at 400X magnification using a charged-couple device (CCD) camera (GW 525EX, Genwac Inc., Orangeburg, NY, USA) attached to a DMLB epifluorescent microscope (Leica Microsystems GmbH, Wetzlar, Germany) with an excitation filter of 490 nm, a 500 nm dichroic filter, and an emission filter of 515 nm. The VisCOMET image analysis software (Impulse Bildanalyse GmbH, Gilching, Germany) was used to analyze the comet images and assess DNA damage. Two

parameters, tail integrated intensity (Singh) and tail moment (Olive) were chosen as the primary indices to quantify DNA damage. The tail moment (Olive) is the product of tail length (distance between the center of the head and tail) and tail DNA percentage (31). Tail integrated intensity (Singh) is an index that incorporates length and breadth of the tail. The algorithm to assess the tail integrated intensity in VisComet starts from the beginning of the tail and examines each vertical scan line until the end of the tail is reached. From each vertical scan line the product of the breadth, position and total intensity is accumulated to obtain 'tail integrated intensity'. Each experiment was repeated three times. One slide was prepared in each replicate and 66 cells were scored from each slide.

***Data analysis of the comet assay to assess DNA damage in Molt-4 and RTN cells.*** The mean of 'tail moment' and 'tail integrated intensity' of the 66 cells in each slide were used in data analysis. Data of 'tail moment' and 'tail integrated intensity' are presented as mean $\pm$  SEM with n=3 for each treatment group. GraphPad Prism 6.03 was also used for statistical analysis. One- or two-way ANOVA followed by the Newman-Keuls multiple comparison tests was used in data analysis. A difference at  $p < 0.05$  was considered statistically significant.

## Results

### *Time-response plots of different concentrations of DHA*

Figure 3 shows the time-dependent growth response to DHA of Molt-4 cells (Figure 3A) and RTN cells (Figure 3B). Dose-dependent growth inhibition by DHA was clearly observed in Molt-4 and RTN cells. Moreover, in control samples (*i.e.* cultures not treated with drug), RTN cells grew significantly faster than Molt-4 cells ( $p < 0.05$ ). Interestingly, DHA was not able to prevent the growth of RTN cells at both 24 h and 48 h point at concentrations of 12.5, 25 and 50  $\mu\text{M}$ . These data showed that RTN cells had acquired resistance to DHA.

### *Dose-responses to DHA of Molt-4 and RTN cells*

To validate whether RTN cells are resistant to DHA, log-dose responses to DHA of Molt-4 and RTN cells at the 24-h and 48-h time points were plotted (Figure 4). At the 24 h time point, the  $\text{IC}_{50}$ s (mean  $\pm$  SD,  $n=3$ ) of DHA for Molt-4 cells and RTN cells were  $15.2 \pm 8.1 \mu\text{M}$  and  $111.6 \pm 14.5 \mu\text{M}$ , respectively. At the 48 h time point, the  $\text{IC}_{50}$ s (mean  $\pm$  SD,  $n=3$ ) of DHA for Molt-4 cells and RTN cells were  $5.8 \pm 1.7 \mu\text{M}$  and  $41.0 \pm 0.2 \mu\text{M}$ , respectively. At the 24-h point, RTN cells had a significantly higher  $\text{IC}_{50}$  value by 7.3-fold than Molt-4 cells ( $p < 0.01$ ) and at the 48-h point, RTN cells also had a significantly higher  $\text{IC}_{50}$  value by 7.1-fold than Molt-4 cells ( $p < 0.0001$ ). Thus, these results confirm that RTN cells had gained resistance to DHA.

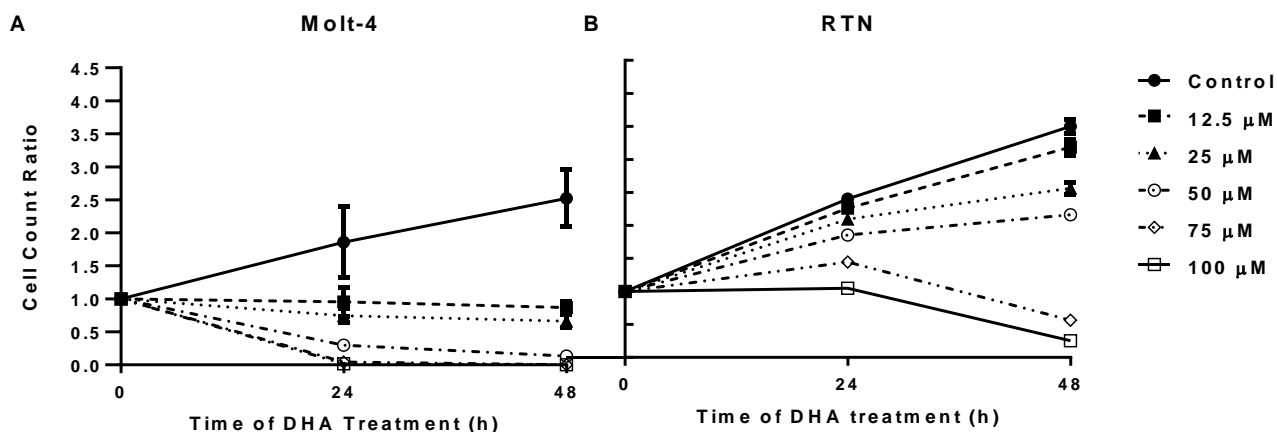


**Figure 3.** Time–response plots for different concentrations of dihydroartemisinin (DHA) of Molt-4 cells (A) and RTN cells (B). Cell count ratio is defined as  $\left(\frac{\text{Cell count at time point}}{\text{Cell count at time zero}}\right)$ .

#### *Dose responses to ART-TF of Molt-4 and RTN cells*

Since RTN cells are not susceptible to DHA, alternative artemisinin derivatives must be tested on RTN cells. Lai *et al* (22) previously reported that ART-TF is more effective than DHA in killing Molt-4 cells. Effectiveness of ART-TF against RTN cells was investigated. Figure 5 shows log dose-responses to ART-TF of Molt-4 cells and RTN cells at the 24-h and 48-h time points. At the 24-h point,  $IC_{50}$  (mean  $\pm$  SD, n=3) of ART-TF on Molt-4 cells and RTN cells were  $2.43 \pm 0.17 \mu\text{M}$  and  $1.85 \pm 0.27 \mu\text{M}$ , respectively. At the 48-h point,  $IC_{50}$  (mean  $\pm$  SD, n=3) of ART-TF on Molt-4 cells and RTN cells were  $0.74 \pm 0.22 \mu\text{M}$  and  $0.54 \pm 0.04 \mu\text{M}$ , respectively. Interestingly at the 24-h time point,  $IC_{50}$  value of ART-TF on RTN cells were significantly lower than the  $IC_{50}$  value of ART-TF on Molt-4 cells ( $p < 0.05$ ). However, there was no significant difference in the  $IC_{50}$  values at the 48-h time point ( $p > 0.05$ ). These results overall showed that RTN cells do not exhibit cross-resistance to ART-TF.

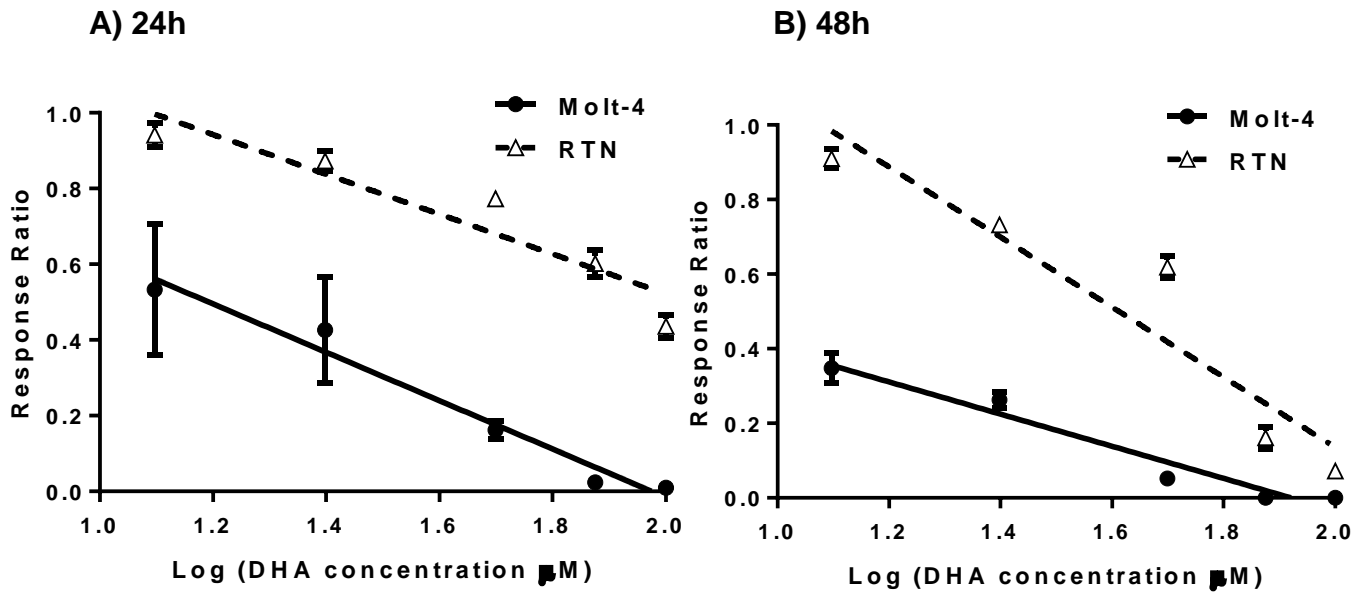


**Figure 4.** Log dose–response plots for Molt-4 cells and RTN cells to dihydroartemisinin (DHA) at the a) 24-h time point, and b) 48-h time point. Graph shows the ratio (mean ± SD, n=3) at different log concentrations of DHA (12.5, 25, 50, 75, and 100 μM). Ratio is defined as

$$\left( \frac{\text{Cell count of drug treated sample}}{\text{Cell count of control}} \right).$$

Since ART-TF and DHA both could induce cytotoxicity by inducing DNA damage, further study was conducted to investigate whether ART-TF can induce more DNA damage both on Molt-4 and RTN cells compared to DHA. The Comet assay was used to measure DNA single-strand breaks in cells.

#### ***Basal and X-ray-induced DNA damage in Molt-4 and RTN cells***

First of all, basal and X-ray-induced (positive control) levels of DNA damage in Molt-4 and RTN cells were assessed by measuring ‘tail moment’ and ‘tail integrated intensity’ (Figure 6).

When comparing the ‘tail moment’ and ‘tail integrated intensity’, Molt-4 cells had significantly

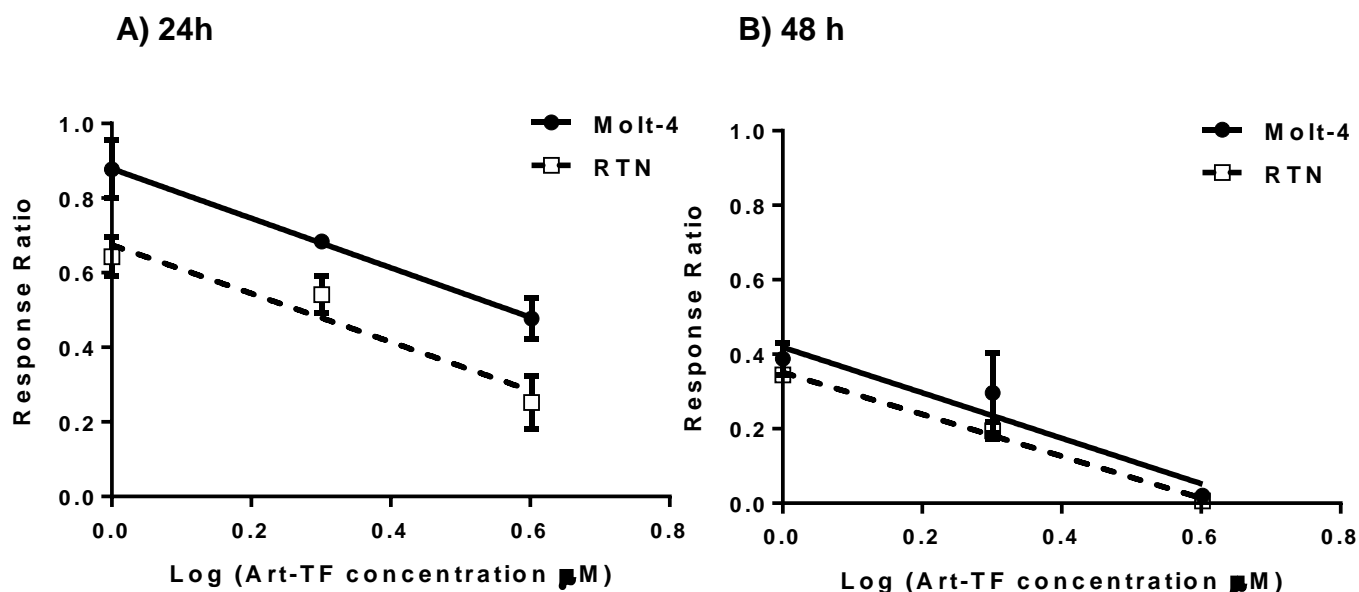
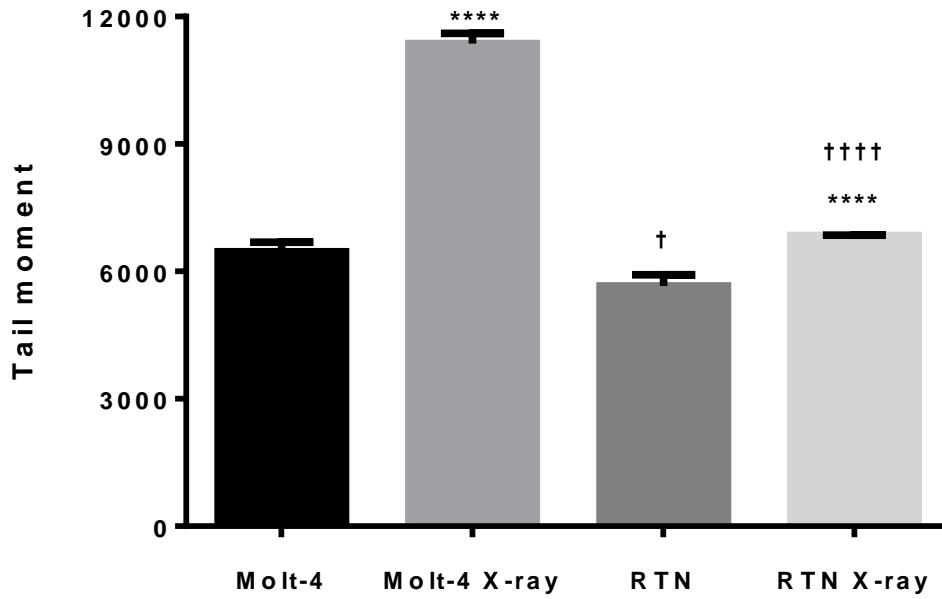


**Figure 5.** Log dose–response plots for Molt-4 cells and RTN cells to artemisinin-tagged holotransferrin (ART-TF) at the a) 24-h time point, and b) 48-h time point. Graph shows the ratio (mean  $\pm$  SD, n=3) at different log concentrations of ART-TF (1, 2, and 4  $\mu\text{M}$ ). Ratio is defined as

$$\left( \frac{\text{Cell count of drug treated sample}}{\text{Cell count of control}} \right).$$

higher DNA damage than RTN cells both under control and x-ray treated conditions (tail moment: control Molt-4 vs. RTN:  $p < 0.05$ , and X-ray: Molt-4 vs. RTN:  $p < 0.0001$ ; tail integrated intensity: control Molt-4 vs. RTN:  $p < 0.05$  and X-ray: Molt-4 vs. RTN:  $p < 0.0001$ ). A two-ANOVA of the data revealed a significant interaction effect ( $p < 0.0001$ ) indicating that Molt-4 and RTN responded differently to X-ray irradiation as quantified by both tail moment and tail integrated intensity. Comet images that closely match each treatment group’s mean ‘tail moment’ and mean ‘tail integrated intensity’ are shown in Figure 7.

A)



B)

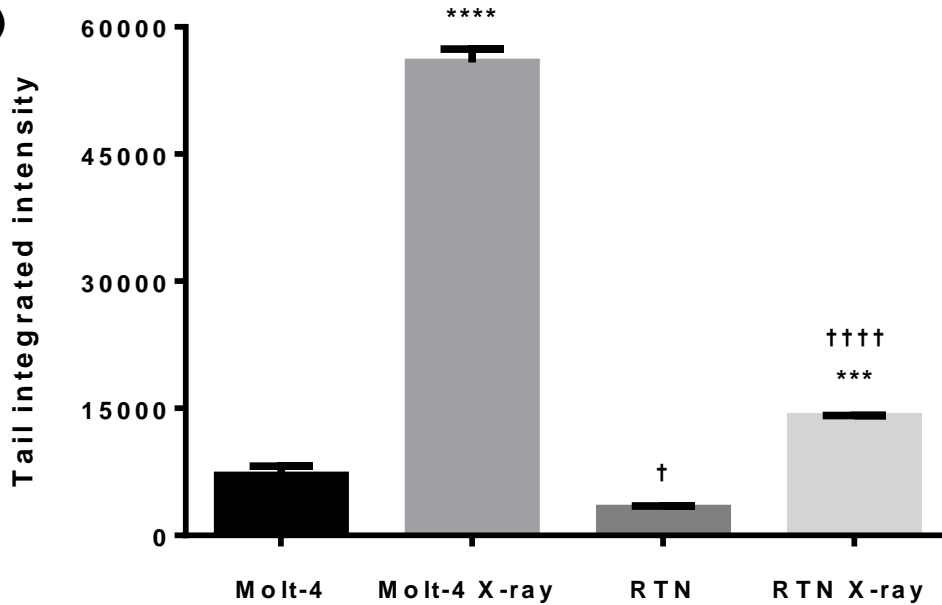


**Figure 6.** Mean ‘tail moment’ (a) and mean ‘tail integrated intensity’ (b) of the four treatment groups: Molt-4 control, X-ray-treated Molt-4, RTN control, and X-ray-treated RTN. Error bars denote SEM. \*\*\* $p < 0.001$ , \*\*\*\* $p < 0.0001$  compared to respective untreated control (Molt-4/RTN) cells; † $p < 0.05$ , compared to Molt-4 control; †††† $p < 0.0001$  compared to Molt-4 X-ray-treated cells.

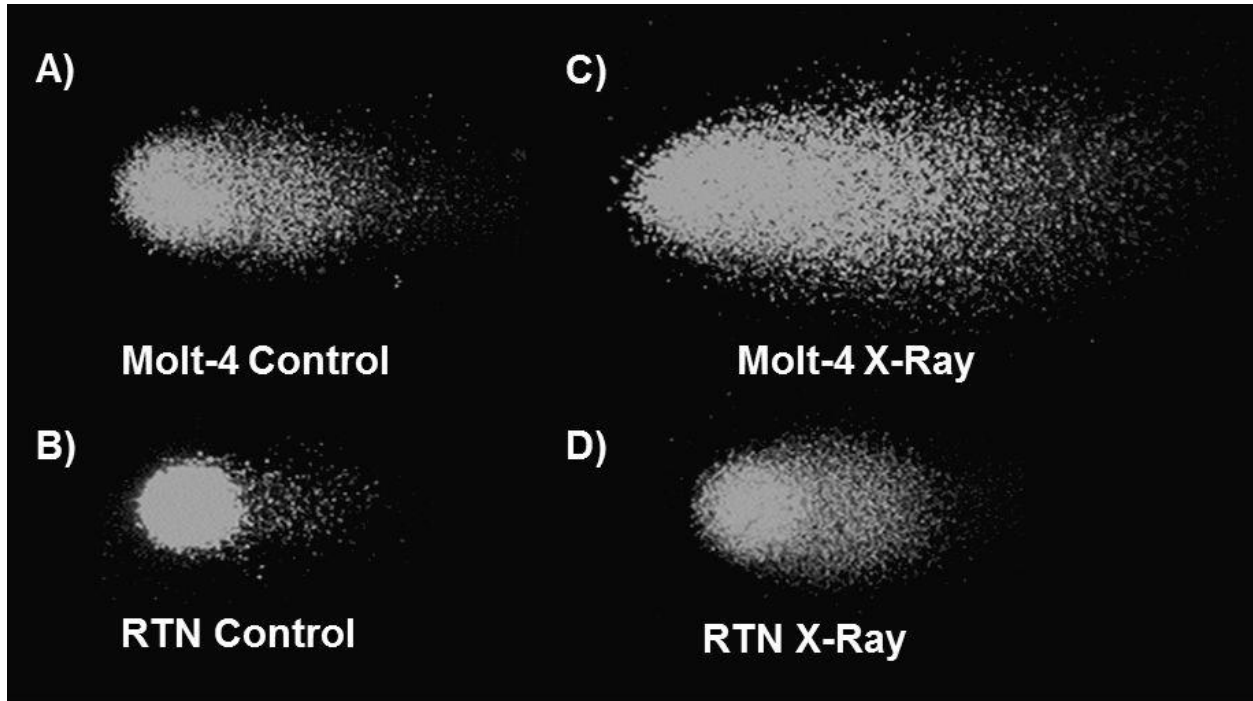


**Figure 7.** Comet images of A) Molt-4 Control, B) RTN Control, C) Molt-4 X-Ray, and D) RTN X-Ray that closely match each treatment's mean 'tail moment' and mean 'tail integrated intensity'. (Magnification 400X, YOYO-1 Dye)

To verify the difference in the degree of cell type-specific DNA damaging effect of DHA and ART-TF in Molt-4 and RTN cells, both Molt-4 and RTN cells were treated with the same concentration (6.2  $\mu\text{M}$ ) of DHA and ART-TF for 24 h. Afterwards, the cells' 'tail moment' and the 'tail integrated intensity' were measured. The cells were not able to be treated for 48 h because when treated with ART-TF on both Molt-4 and RTN cells, all the cells were completely dead and were not available for Comet assay analysis.



### ***DNA damaging effect of DHA and ART-TF on Molt-4 cells***

In Molt-4 cells, significant DNA damage was induced both by DHA and ART-TF compared to the untreated control (Figure 8). ART-TF was able to cause more DNA damage compared to DHA in Molt-4 cells as shown by the 'tail moment' and 'tail integrated intensity' (tail moment: control vs. DHA:  $p < 0.05$ , control vs. ART-TF:  $p < 0.01$ ; DHA vs. Art-TF:  $p < 0.05$ ; tail integrated intensity: control vs. DHA:  $p < 0.01$ , control vs. ART-TF:  $p < 0.0001$ , DHA vs. ART-TF:  $p < 0.001$ ). Comet images that closely match each treatment group's mean 'tail moment' and mean 'tail integrated intensity' are shown in Figure 9.

### ***DNA damaging effect of DHA and ART-TF on RTN cells***

In RTN cells, there was no significant difference ( $p > 0.05$ ) in the 'tail moment' and 'tail integrated intensity' between untreated and DHA-treated cells (Figure 10). However, ART-TF induced significantly greater DNA damage as assessed by 'tail moment' and 'tail integrated intensity' when compared to untreated and DHA- treated RTN cells (tail moment: control vs. ART-TF:  $p < 0.01$ , DHA vs. ART-TF:  $p < 0.05$ ; tail integrated intensity: control vs. ART-TF:  $p < 0.001$ , DHA vs. ART-TF:  $p < 0.01$ ). Overall, DHA did not cause a significant change in DNA damage. However, ART-TF was able to increase the level of DNA damage in RTN cells. Comet images that closely match each treatment group's mean 'tail moment' and mean 'tail integrated intensity' are shown in Figure 11.

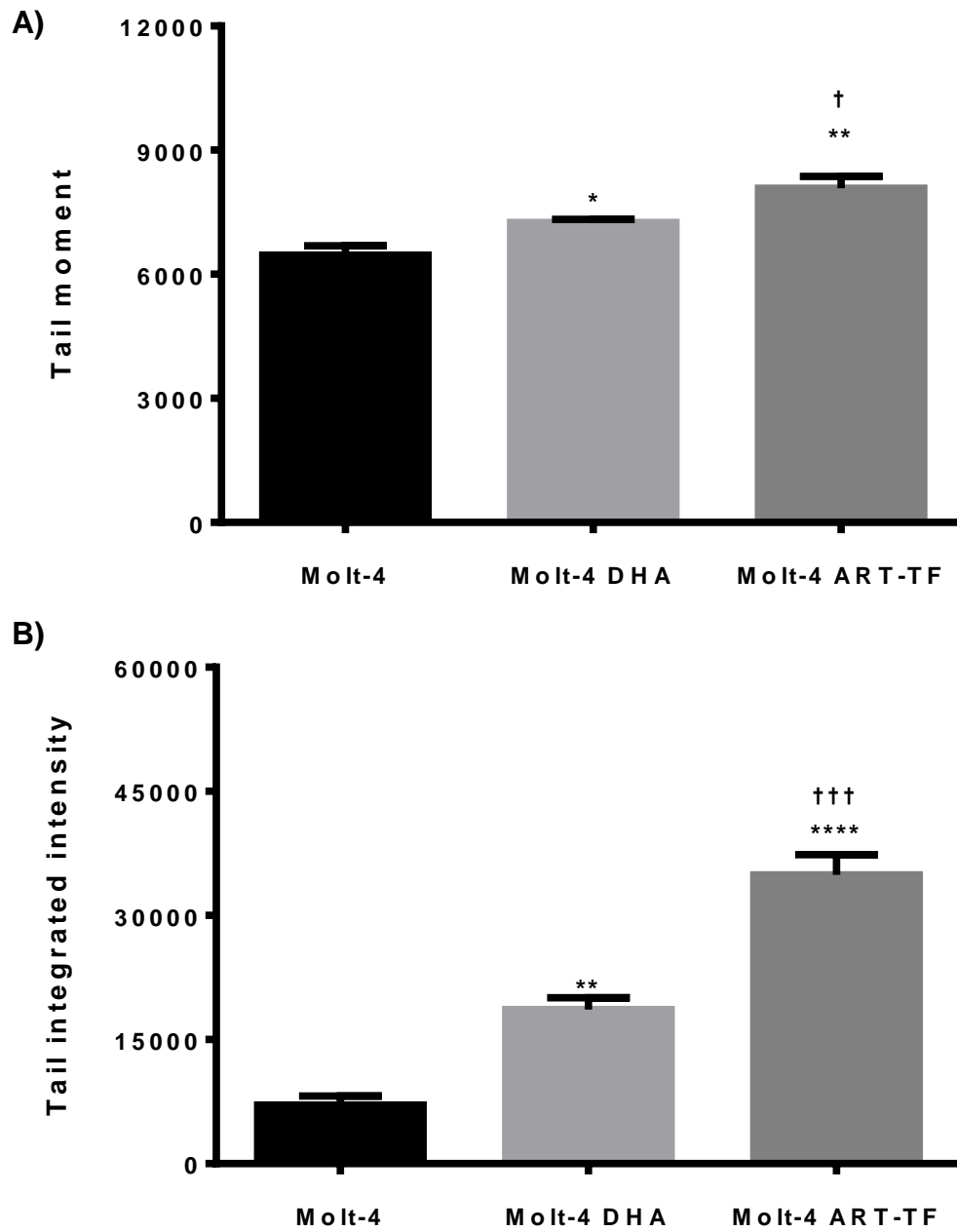


**Figure 8.** Mean ‘tail moment’ (a) and mean ‘tail integrated intensity’ (b) of Molt-4 control cells and Molt-4 cells treated with 6.2 μM dihydroartemisinin (DHA) or 6.2 μM of artemisinin-tagged holotransferrin (ART-TF) for 24 h. Error bars denote SEM. \* $p < 0.05$ , \*\* $p < 0.01$ , \*\*\*\* $p < 0.0001$  compared to Molt-4 control cells; † $p < 0.05$ ; ††† $p < 0.001$  compared to DHA-treated Molt-4 cells.

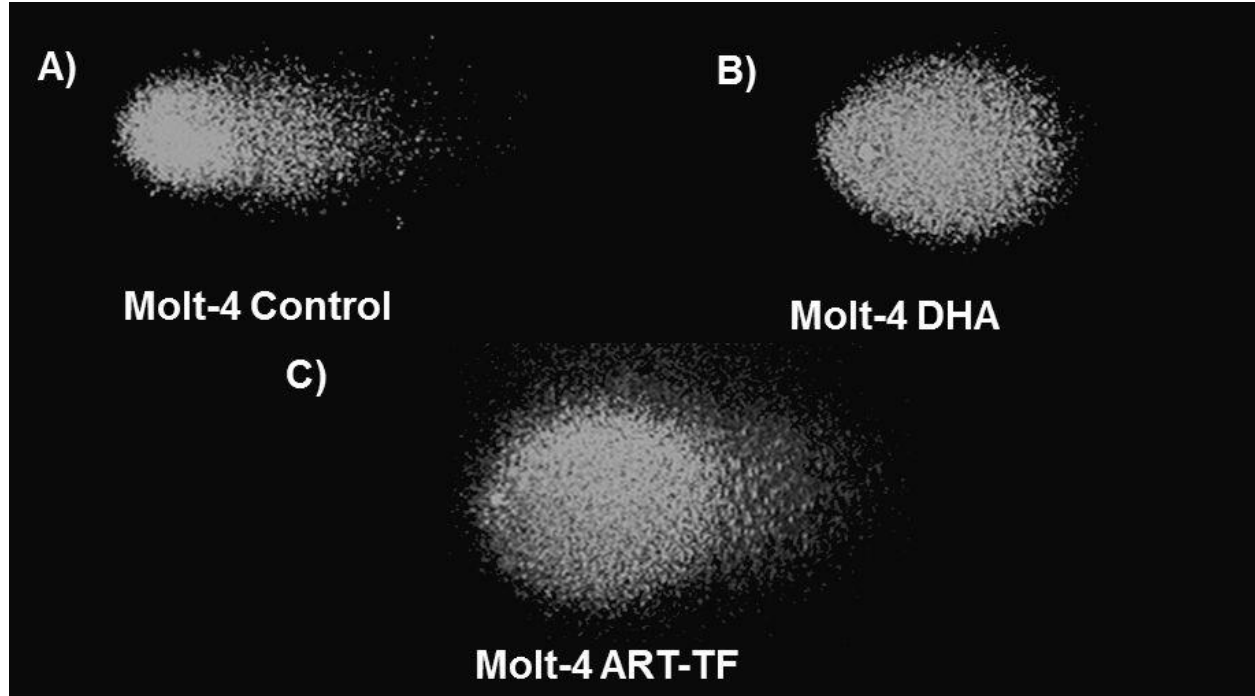


**Figure 9.** Comet images of A) Molt-4 Control, B) Molt-4 DHA and C) Molt-4 ART-TF that closely match each treatment's mean 'tail moment' and mean 'tail integrated intensity'. (Magnification 400X, YOYO-1 Dye)

## Discussion

In this study, a DHA-resistant Molt-4 cell line termed RTN was established. There has been a previous report by Lu *et al* of a DHA-resistant colon carcinoma cell line (HCT116/R) after 45 exposure cycles to DHA (32). Colon carcinoma cells were exposed to increment concentrations of DHA for 72 h each before a washing process in between. The  $IC_{50}$  of the resulting HCT116/R was 4.3 times higher than that of the parental colon carcinoma cells. In the present research, Molt-4 cells were exposed to 25, 50, 75, and 100  $\mu$ M of DHA for three 24-h cycles for each concentration, with total of 12 cycles.

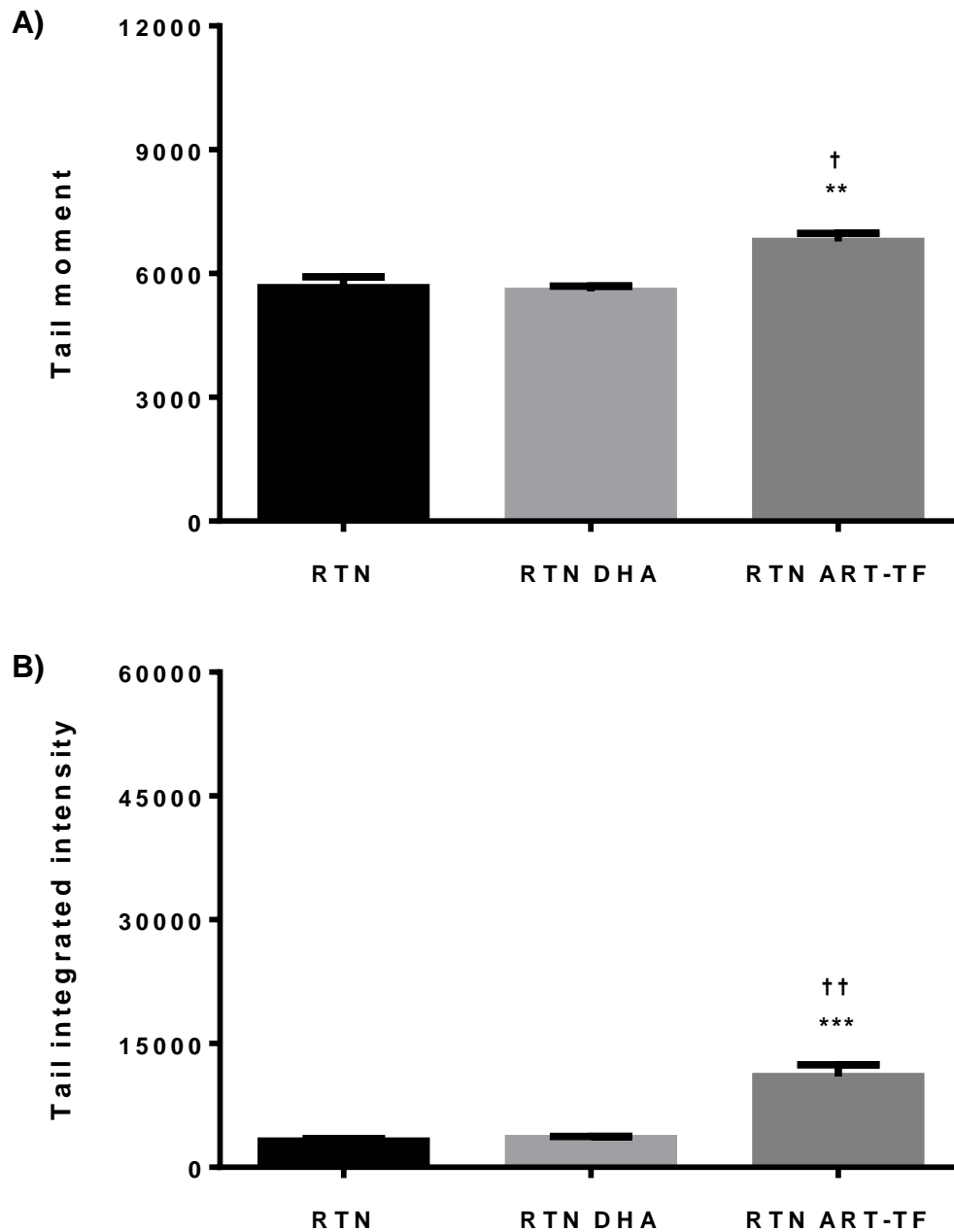


**Figure 10.** Mean ‘tail moment’ (a) and mean ‘tail integrated intensity’ (b) of RTN control cells and RTN cells treated with 6.2  $\mu$ M dihydroartemisinin (DHA) or 6.2  $\mu$ M of artemisinin-tagged holotransferrin (ART-TF) for 24h. Error bars denote SEM. \*\* $p$ <0.01, \*\*\* $p$ <0.0001 compared to RTN control cells; † $p$ <0.05; †† $p$ <0.01 compared to DHA-treated RTN cells.

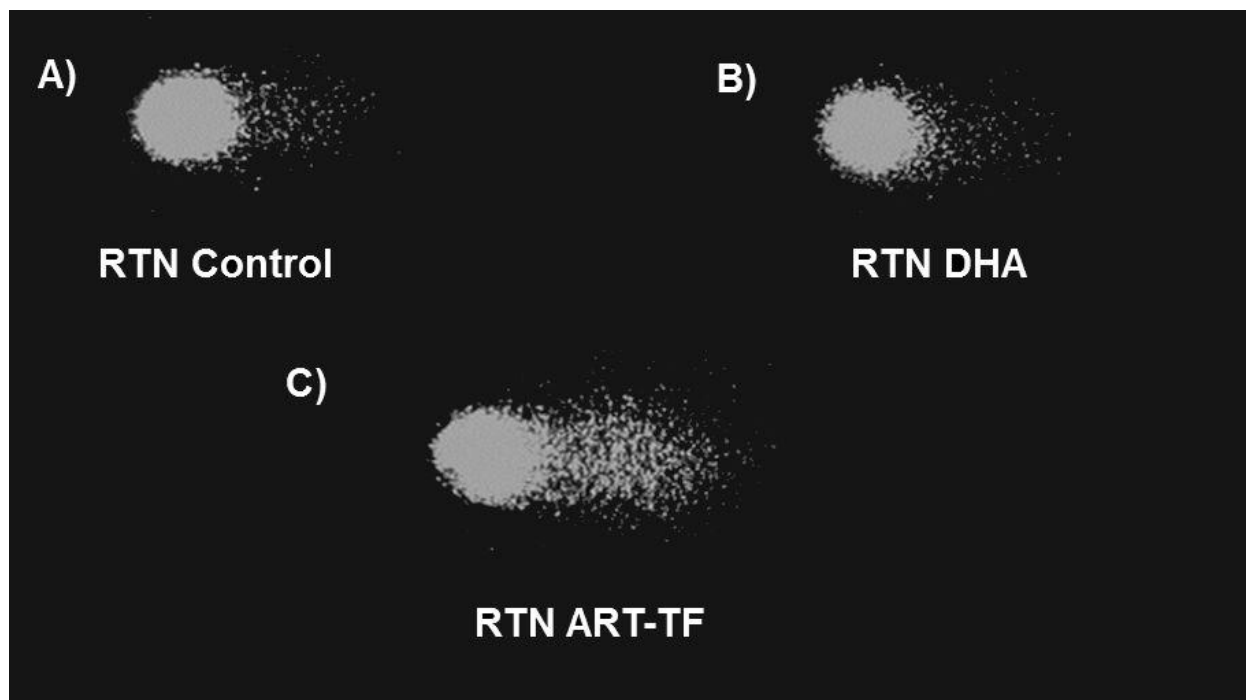


**Figure 11.** Comet images of A) RTN Control, B) RTN DHA and C) RTN ART-TF that closely match each treatment's mean 'tail moment' and mean 'tail integrated intensity'. (Magnification 400X, YOYO-1 Dye)

In the RTN cell, there was a 7.3 fold and 7.1 fold increases in  $IC_{50}$  at the 24-h and the 48-h time points, respectively. There is a possibility that different cancer cell lines would have different vulnerabilities to drug-resistance development. Bachmeier *et al* (33) previously reported that after 24 h of incubation with artesunate, a semisynthetic derivative of artemisinin, artesunate resistance developed in MDA-MD-231 but not in the MDA-MB-468 breast cancer cell lines. Moreover, Sadava *et al.* (34) reported two small cell lung cancer cell lines have different susceptibilities to artemisinin. The  $IC_{50}$  of artemisinin for cell line H69VP was 10 fold higher than that for the other cell line H69. Fascinatingly, prior treatment of the cells with transferrin enabled effective killing of the H69VP lung cancer cell line.

It is interesting to observe that RTN's cell count ratio increased faster than that of the Molt-4 cells. There could be two possible explanations for this finding: RTN cells might have a higher cell division rate; or they might have a decreased tendency to die, e.g., via apoptosis. Since cells that divide at a higher rate should be more susceptible to the toxicity of DHA, the second explanation seems more plausible.

Lai *et al* (22) demonstrated that ART-TF is a more powerful compound in killing Molt-4 cells. As postulated, it was confirmed that RTN cells were also more susceptible to ART-TF than DHA. When comparing the IC<sub>50</sub> values, ART-TF was significantly more potent than DHA by 60-fold ( $p < 0.0001$ ) and 76-fold ( $p < 0.0001$ ) at the 24-h and 48-h time points, respectively.

It is interesting to observe that RTN cells demonstrated resistance to DHA but not to ART-TF. These findings may imply that DHA and ART-TF have different mechanisms of action to cause cytotoxicity. DHA would probably enter the cells by simple membrane diffusion and can reach organelles such as the mitochondria and generate apoptosis. However, ART-TF is transported into cells *via* receptor-mediated endocytosis (35). Its cytotoxicity would probably be correlated to membrane damage in endosome, plasma membrane, and lysosome.

Previously, Li *et al.* (36) found that artesunate induced DNA damage in VC8 cell line, derived from the V79 Chinese hamster lung fibroblast cell line and Berdelle *et al.* (37) reported that artesunate induced DNA damage in the human glioblastoma cell line LN-229 as measured by the Comet assay using tail moment as the parameter for DNA damage. In this study, the Comet assay was used to determine DNA damage in Molt-4 and RTN cells, and investigated the level of DNA damage triggered by DHA and ART-TF. This is the first time that the level of DNA damage in an artemisinin-resistant cancer cell line was studied.

The Comet assay results revealed that compared to Molt-4 cells, RTN cells were more resistant to DNA damage both in normal state and under X-ray irradiation. This may be due to an enhanced DNA repair capability in RTN cells or chromatin DNA in RTN cells might be more tightly packed by forming a DNA-histone complex to protect DNA from damage induced by x-ray irradiation or other chemotherapeutic agents (38, 39).

However, there was not significant DHA-induced DNA damage in the RTN cells. In accordance with the increase in cytotoxicity  $IC_{50}$  value of DHA on RTN cells, RTN cells were resistant to DHA in terms of DNA damage as well. The reason for this may be RTN cells' reduced intracellular DHA due to efflux mediated by cell surface transporters (40) or elevated levels of molecules and enzymes that reduce DHA-generated reactive oxidative species (41,42).

It is interesting to note that RTN cells are resistant to DHA but vulnerable to ART-TF in terms of DNA damage. As shown that ART-TF is more potent in killing RTN cells compared to DHA in terms of  $IC_{50}$  values, the Comet assay results also verify that ART-TF is a more effective anti-cancer agent compared to DHA. Due to the fact DHA penetrates into the cell by simple diffusion while ART-TF is transported in to the cells via transferrin-receptor, ART-TF would be more difficult to be removed by the RTN cells.

## **Conclusion**

In this study, DHA-resistant Molt-4 lymphoblastoid cell line termed RTN cell line has been developed for the first time. RTN cell line has faster growth rate and exhibit resistance to DHA compared to the parent Molt-4 cell line. Moreover, RTN cell's basal and X-ray induced DNA

damage levels were significantly lower than those of Molt-4 cells and showed no DHA-induced DNA damage.

However, synthetic artemisinin derivative ART-TF exhibited significant cytotoxic effect in terms of both  $IC_{50}$  values and DNA damage level. Further molecular studies will be needed to determine the precise mechanisms on how ART-TF kills DHA-resistant RTN cells.

Hence, in the use of artemisinin and its derivatives for cancer treatment, compounds with different mechanisms of action or different chemical structures can be used to circumvent development of resistance in cancer cells and effectively kill drug-resistant cancer cells.

## **Acknowledgment**

ART-TF used in this research was provided by Professor Tomikazu Sasaki of the Department of Chemistry, University of Washington.

## **Copyright Note**

Many figures and texts within this Master's thesis have been taken with permission from earlier publications of this work in the journal Anticancer Research by this author (43, 44).



## References

- 1 Li Y and Wu YL: An over four millennium story behind ginghamosu (artemisinin)- a fantastic antimalarial drug from a traditional Chinese herb. *Curr Med Chem* 10: 2197-2230, 2003.
- 2 Singh NP and Lai HC: Selective toxicity of dihydroartemisinin and holotransferrin toward human breast cancer cells. *Life Sci* 70: 49-56, 2001.
- 3 Jiao Y, Ge CM, Meng QH, Cao JP, Tong J and Fan SJ: Dihydroartemisinin is an inhibitor of ovarian cancer cell growth. *Acta Pharmacol Sinica* 28: 1045-1056, 2008.
- 4 Efferth T, Dunstan H, Sauerbrey A, Miyachi H and Chitambar CR: The antimalarial artesunate is also active against cancer. *Intl J Oncol* 18: 767-783, 2001.
- 5 Moore JC, Lai H, Li J, McDougall JA, Singh NP and Chou CK: Oral administration of dihydroartemisinin and ferrous sulfate retarded implanted fibrosarcoma growth in the rat. *Cancer Lett* 91: 83-87, 1995.
- 6 Singh NP, Lai HC, Park JS, Gerhardt TE, Kim BJ, Wang S and Sasaki T: Effects of artemisinin dimers on rat breast cancer cells *in vitro* and *in vivo*. *Anticancer Res* 31: 4111-4114, 2011.
- 7 Singh NP and Verma KB: Case report of a laryngeal squamous cell carcinoma treated with artesunate. *Arch Onc* 10: 279-280, 2002.
- 8 Singh NP and Panwar VK: Case report of a pituitary macroadenoma treated with artemether. *Integr Cancer Ther* 5: 391-394, 2006.
- 9 Singh NP and Lai HC: Artemisinin induces apoptosis in human cancer cells. *Anticancer Res* 24: 2277-2280, 2004.
- 10 O'Neill PM, Barton VE and Ward SA: The molecular mechanism of action of artemisinin- the debate continues. *Molecules* 15: 1413-1422, 2010.

- 11 Andrews NC: Iron homeostasis: insights from genetics and animal models. *Nat Rev Genet* 1: 208-217, 2000.
- 12 Karin M and Mintz B: Receptor-mediated endocytosis of transferrin in developmentally totipotent mouse teratocarcinoma stem cells. *J Biol Chem* 256: 3245-3252, 1981.
- 13 May WS and Cuatrecasas P: Transferrin receptor: its biological significance. *J Membr Biol* 88: 205-215, 1985.
- 14 Vendrik CJ, Bergers JJ, De Jong WH, and Steerenberg P: Resistance to cytostatic drugs at the cellular level. *Cancer Chemother Pharmacol* 29: 413-429, 1992.
- 15 Ambudkar SV, Dey S, Hrycyna CA, Ramachandra M, Pastan I, and Gottesman MM: Biochemical, cellular, and pharmacological aspects of the multidrug transporter. *Ann Rev Pharmacol Toxicol* 39: 361-398, 1999.
- 16 Sethi T, Rintoul RC, Moore SM, MacKinnon AC, Salter D, Choo C, Chilvers ER, Dransfield I, Donnelly SC, Strieter R and Haslett C: Extracellular matrix proteins protect small cell lung cancer cells against apoptosis: A mechanism for small cell lung cancer growth and drug resistance *in vivo*. *Nat Med* 5: 662-668, 1999.
- 17 Morin PJ: Drug resistance and the microenvironment: nature and nurture. *Drug Resist Update* 6: 169-172, 2003.
- 18 Salehan MR, Morse HR: DNA damage repair and tolerance: a role in chemotherapeutic drug resistance. *Br J Biomed Sci* 70: 31- 40, 2013.
- 19 McKenna DJ, McKeown SR and McKelvey-Martin VJ: Potential use of the comet assay in the clinical management of cancer. *Mutagenesis* 23: 183-190, 2008.
- 20 Lu JJ, Chen SM, Ding J and Meng LH: Characterization of dihydroartemisinin-resistant colon carcinoma HCT166/R cell line. *Mol Cell Biochem* 360: 329-337, 2012.

- 21 Lai HC, Singh NP and Sasaki T: Development of artemisinin compounds for cancer treatment. *Invest New Drugs* 31: 230-246, 2013.
- 22 Lai H, Sasaki T, Singh NP and Messay A: Effects of artemisinin-tagged holotransferrin on cancer cells. *Life Sci* 76: 1267-1279, 2005.
- 23 McKenna DJ, McKeown SR and McKelvey-Martin VJ: Potential use of the comet assay in the clinical management of cancer. *Mutagenesis* 23: 183-190, 2008.
- 24 Ostling O and Johansson KJ: Microelectrophoretic study of radiation-induced DNA damages in individual mammalian cells. *Biochem Biophys Res Commun* 123: 291-298, 1984.
- 25 Singh NP, McCoy MT, Tice RR and Schneider EL: A simple technique quantification of low levels of DNA damages in individual cells. *Exp Cell Res* 175: 184-191, 1988.
- 26 Singh NP and Stephens RE: Microgel electrophoresis: sensitivity, mechanisms and DNA electrostretching. *Mutat Res* 12: 167-175, 1997
- 27 Kim BJ and Sasaki T: Synthesis of O-aminodihydroartemisinin via TMS triflate catalyzed C-O coupling reaction. *J Org Chem* 69: 3242-3244, 2004.
- 28 Krauth J: Nonparametric analysis of response curves. *J Neurosci Method* 2: 239-252, 1980.
- 29 Tice RR, Andrews PW and Singh NP: The single cell gel assay: a sensitive technique for evaluating intercellular differences in DNA damage and repair. *Basic Life Sci* 53: 291-301, 1990.
- 30 Kreig Jr EF, Mathias PI, Toennis CA, Clark JC, Marlow KL, B'Hymer C, Singh NP, Gibson RL and Butler MA: Detection of DNA damage in workers exposed to JP-8 jet fuel. *Mutat Res* 747: 218 -227, 2012.

- 31 Olive P and Banáth JP: Induction and rejoining of radiation induced DNA single strand breaks: “tail moment” as a function of position in the cell cycle. *Mutat Res* 294: 275-283, 1993.
- 32 Lu JJ, Meng LH, Shankavaram UT, Zhu CH, Tong LJ, Chen G, Lin LP, Weinstein JN and Ding J: Dihydroartemisinin accelerates c-MYC oncoprotein degradation and induces apoptosis in c-MYC overexpressing tumor cells. *Biochem Pharmacol* 80: 22-30, 2010.
- 33 Bachmeier B, Fichtner I, Killian PH, Kronski E, Pfeffer U and Efferth T: Development of resistance towards artesunate in MDA-MB-231 human breast cancer cells. *PLoS One* 6: e20550, 2011.
- 34 Sadava D, Phillips T, Lin C and Kane SE: Transferrin overcomes drug resistance to artemisinin in human small-cell lung carcinoma cells. *Cancer Lett* 179: 151-156, 2002.
- 35 Nakase I, Gallis B, Takatani-Nakase T, Oh S, Lacoste E, Singh NP, Goodlet DR, Tanaka S, Futaki S, Lai H and Sasaki T: Transferrin receptor-dependent cytotoxicity of artemisinin-transferrin conjugates on prostate cancer cells and induction of apoptosis. *Cancer Lett.* 274: 290-298, 2009.
- 36 Li PC, Lam E, Roos WP, Zdzienicka MZ, Kaina B and Efferth T: Artesunate derived from traditional Chinese medicine induces DNA damage and repair. *Cancer Res.* 68: 4347-4351, 2008.
- 37 Berdelle N, Nikolova T, Quiros S, Efferth T and Kaina B: Artesunate induces oxidative DNA damage, sustained DNA double-strand breaks and the ATM/ATR damage response in cancer cells. *Mol Cancer Ther* 10: 2224-2233, 2011.
- 38 Ljungman M and Hanawalt PC: Efficient protection against oxidative DNA damage in chromatin. *Mol Carcinog.* 5: 264-260, 1992.

- 39 Chiu S and Oleinick NL: Radioprotection against the formation of DNA double-strand breaks in cellular DNA but not native cellular chromatin by the polyamine spermine. *Radiat Res.* 76: 749-756, 2000.
- 40 Aouida M, Poulin R and Ramotar D: The human carnitine transporter SLC22A16 mediates high affinity uptake of the anticancer polyamine analogue bleomycin-A5. *J Biol Chem* 26: 6275-6284, 2010
- 41 Yen HC, Li SH, Majima HJ, Huang YH, Chen CP, Liu CC, Tu YC and Chen CW: Up-regulation of antioxidant enzymes and coenzyme Q(10) in a human oral cancer cell line with acquired bleomycin resistance. *Free Radic Res* 45: 707-716. 2011.
- 42 Cort A, Timur M, Dursun E, Kucuksayan E, Aslan M and Ozben T: Effects of N-acetylcystein on bleomycin-induced apoptosis in malignant testicular germ cell tumors. *J Physiol Biochem* 68: 555-562.2012.
- 43 Park J, Lai HC, Singh M, Sasaki T and Singh NP: Development of a dihydroartemisinin-resistant Molt-4 leukemia cell line. *Anticancer Res* 34: 2807-2810, 2014.
- 44 Park J, Lai HC, Sasaki T and Singh NP: DNA damage in dihydroartemisinin-resistant Molt-4 cells. *Anticancer Res* 35: 1339-1343. 2015.